Viscous flux motion in a Josephson-coupled layer model of high-T_c superconductors

John R. Clem and Mark W. Coffey
Ames Laboratory—U.S. Department of Energy and Department of Physics, Iowa State University, Ames, Iowa 50011
(Received 19 April 1990)

We develop and apply a theory for the structure of an isolated vortex parallel to the layers in a Josephson-coupled layer model of a high-T_c copper oxide superconductor. This model takes into account the discreteness of the copper oxide planes, which is expected to become important below the crossover temperature where the coherence length $\xi_c(T)$ becomes less than the lattice constant c. We apply the layer model to the motion of a vortex parallel to the planes and calculate the viscous drag coefficient. This result is contrasted with that of the anisotropic Bardeen-Stephen model.

I. INTRODUCTION

The high-T_c copper oxide superconductors are well known to have anisotropic magnetic properties. In a compound like $YBa_2Cu_3O_{7-\delta}$ the magnetic properties are very similar (although not exactly the same) in the a and b directions, parallel to the CuO_2 layers, but quite different in the c direction perpendicular to the layers. It has been customary to describe the high-T_c copper oxide materials within the framework of anisotropic Ginzburg-Landau theory, in which an effective-mass tensor is employed.[1-8] In a reference frame aligned with the principal axes, this mass tensor is diagonal, and the diagonal elements m_i $(i=1,2,3=a,b,c)$ are normalized[7,8] such that $m_1m_2m_3=1$. The penetration depths $\lambda_i=\lambda\sqrt{m_i}$ describe the decay of components of the supercurrent pointing along the principal directions, and the corresponding coherence lengths $\xi_i=\xi/\sqrt{m_i}$ characterize the spatial variation of the order parameter along these directions. The Ginzburg-Landau parameter $\kappa=\lambda/\xi$ is defined in terms of the scalars $\lambda=(\lambda_1\lambda_2\lambda_3)^{1/3}$ and $\xi=(\xi_1\xi_2\xi_3)^{1/3}$. We note that for a copper oxide high-T_c material, the smallest length scale in the anisotropic Ginzburg-Landau description is ξ_c.

We briefly touch on how the parameters ξ_i of the anisotropic Ginzburg-Landau theory are measured. The coherence lengths ξ_a, ξ_b, and ξ_c are usually inferred from measurements of the upper critical fields B_{c2i} at temperatures near T_c, with $B_{c2a}=\phi_0/2\pi\xi_b\xi_c$, $B_{c2b}=\phi_0/2\pi\xi_a\xi_c$, and $B_{c2c}=\phi_0/2\pi\xi_a\xi_b$ being the critical fields along the a, b, and c axes, respectively. The Ginzburg-Landau theory is expected to be valid only in a certain temperature range close to T_c. The temperature must be close enough to T_c for the theory to be valid, where $\xi_i(T)$ is much larger than the corresponding lattice parameter. On the other hand, the temperature cannot be too close to T_c, since otherwise critical thermodynamic fluctuations arise.

Measured temperature derivatives of B_{c2i} at $T=T_c$ commonly have been used in conjunction with the Werthamer-Helfand-Hohenberg dirty-limit formula[9] $B_{c2}(0)=0.693|\partial B_{c2}/\partial T|_{T_c}T_c$ to obtain values for the upper critical fields extrapolated to zero temperature $B_{c2i}(0)$. In turn, the coherence lengths extrapolated to zero temperature $\xi_i(0)$ have been obtained from $B_{c2a}(0)=\phi_0/2\pi\xi_b(0)\xi_c(0)$, $B_{c2b}(0)=\phi_0/2\pi\xi_a(0)\xi_c(0)$, and $B_{c2c}(0)=\phi_0/2\pi\xi_a(0)\xi_b(0)$. Using this procedure, the authors of Ref. 10, for example, found $\xi_a(0)=\xi_b(0)=16$ Å and $\xi_c(0)=3$ Å for single crystals of $YBa_2Cu_3O_{7-\delta}$.

For isotropic superconductors, a simple model for the viscous drag coefficient, which generally is in good agreement with experiments, is due to Bardeen and Stephen (BS).[11] In their model, the dissipation occurs inside and in the immediate vicinity of the vortex core, approximated as a normal core of radius ξ. Anisotropy can be incorporated into the BS calculation by use of the same effective-mass tensor as used in the Ginzburg-Landau theory.[12] The smallest length scale in this theory is $\xi_c(T)$, and a calculation of the viscous drag coefficient that results in an expression involving ξ_c is not expected to be valid for temperatures below the crossover temperature[5,13,14] where $\xi_c(T)<c$, the lattice parameter in the c direction. In particular, at low temperature, the anisotropic BS theory cannot be expected to give the correct expression for the viscous drag coefficient for a vortex parallel to the CuO_2 layers, moving parallel to these layers.

Viscous flux motion in anisotropic type-II superconductors has been considered, e.g., in Refs. 15 and 16. Using a simple microscopic theory for energy dissipation, these authors have discussed a phenomenological theory of vortex motion and flux flow resistivity.

In this paper we calculate the viscous drag coefficient η for a vortex in a microscopically layered high-T_c superconductor, the vortex being parallel to the a axis, and moving in the b direction under the influence of an applied driving current in the c direction (see Fig. 1). For this geometry, according to the anisotropic BS theory, the flux flow resistivity should vary approximately as $\rho_f\simeq\rho_c(B/B_{c2a})$, where ρ_c is the normal-state resistivity along the c direction. By equating the Lorentz force per unit length of vortex to the viscous drag force per unit length, the anisotropic BS model in the dirty limit gives,

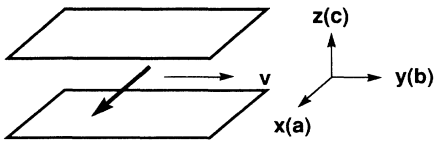

FIG. 1. Geometry for the calculation of the viscous drag coefficient. The vortex (bold arrow) is parallel to the a axis and moves with velocity $\mathbf{v}$ (arrow) in the b direction under the influence of an applied driving current in the c direction. Shown in the sketch are two superconducting layers.

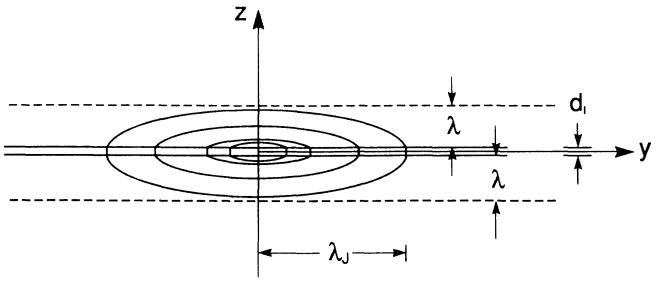

FIG. 2. Sketch of the supercurrent distribution about a vortex in the insulating barrier of a single Josephson junction. The various penetration depths are indicated, and typically $\lambda_J \gg \lambda$. The London penetration depth λ gives the length scale over which the magnetic field enters the superconductors and, correspondingly, the scale over which the supercurrents decay in the superconductors. The Josephson penetration depth λ_J gives the length scale over which the gauge-invariant phase difference varies and, therefore, over which the Josephson tunneling current varies.

for this vortex orientation, current direction and direction of motion,[12] $\eta=\phi_0^2/2\pi\xi_b\xi_c c^2\rho_c$. This expression is expected to be valid for temperatures close to T_c and for low magnetic field. In the BS model, the dissipation that contributes to the viscous drag is concentrated in the vicinity of the vortex core. We see that the above expression involves the cross-sectional dimensions $(\xi_b\xi_c)$ of the vortex core region. We anticipate that if the vortex core region has altered behavior at low temperature due to the atomic scale discreteness of the superconductor's structure, then the corresponding expression for the viscous drag coefficient is also altered.

This paper proceeds as follows. We first review (a) the core structure of a straight vortex threading through the insulating barrier of a Josephson junction and (b) the calculation of the viscous drag coefficient when such a vortex moves through the insulating region. Next, we develop the theory for the vortex structure in a Josephson-coupled layer model of a high-T_c superconductor. This model takes into account the discreteness of the copper oxide planes, which is expected to be important when $\xi_c(T)$ is less than the lattice parameter c. We then apply this description to compute the viscous drag coefficient η.

II. VORTEX STRUCTURE IN A JOSEPHSON JUNCTION AND VISCOUS DRAG COEFFICIENT

We briefly review some of the characteristics of an isolated, singly quantized magnetic vortex in the insulating region of a single Josephson junction and then indicate how the viscous drag on such a vortex, moving parallel to the plane of the junction, can be calculated. We use the geometry of Fig. 2, with the insulating barrier, of thickness d_i, in the x-y plane. For the sake of simplicity we take the superconductors to be isotropic and of the same material. Then the basic relations governing the magnetic and electric fields in the junction are[17–20]

$$\frac{\partial\Delta\gamma}{\partial x}=\frac{2ed}{\hbar c}b_y\ ,$$
$$\frac{\partial\Delta\gamma}{\partial y}=-\frac{2ed}{\hbar c}b_x\ , \tag{2.1}$$
$$\frac{\partial\Delta\gamma}{\partial t}=\frac{2ed_i}{\hbar}E\ .$$

Here $\Delta\gamma$ is the gauge-invariant phase difference across the junction and the magnetic thickness $d=2\lambda+d_i$, assuming that the superconductors have thicknesses much larger than the London penetration depth λ. The penetration depth λ gives the scale over which the magnetic field enters the superconductors and, correspondingly, the scale over which the supercurrents decay in the superconductors.

Along with (2.1) we have the Josephson tunneling current relation $J_z=J_0\sin\Delta\gamma$, where J_0 is a temperature-dependent amplitude (the maximum Josephson current density). Equation (2.1), together with the Josephson current relation and Maxwell's equation including the displacement current, yields the two-dimensional (2D) sine-Gordon equation

$$\frac{\partial^2\Delta\gamma}{\partial x^2}+\frac{\partial^2\Delta\gamma}{\partial y^2}-\frac{1}{\bar{c}^2}\frac{\partial^2\Delta\gamma}{\partial t^2}=\frac{1}{\lambda_J^2}\sin\Delta\gamma\ , \tag{2.2}$$

where $\bar{c}^2\equiv c^2/4\pi dC$, C is the junction capacitance per area, and $\lambda_J^2\equiv\hbar c^2/8\pi edJ_0$. Equation (2.2) is a nonlinear wave equation for the gauge-invariant phase difference which does not contain any dissipative terms. For the calculation of the viscous drag coefficient below, we assume that these terms can be ignored to leading order. A mathematical justification for this procedure is provided by the perturbation treatment of Ref. 21. In Eq. (2.2) the quantity $\bar{c}$ gives the speed of electromagnetic radiation in the barrier, and λ_J is the Josephson penetration depth. We recall that $\omega_J=\bar{c}/\lambda_J$ is the angular frequency of longitudinal plasma waves in the insulating barrier. The Josephson penetration depth gives the length scale over which the gauge-invariant phase difference varies and, therefore, over which the Josephson tunneling current varies. The supercurrent distribution about a vortex in the insulating region of a single Josephson junction is sketched in Fig. 2. The various penetration depths are indicated in Fig. 2 and we note that typically $\lambda_J\gg\lambda$.

The sine-Gordon equation (2.2) has been well studied and is known to possess many special properties. The single soliton solution of (2.2) is identified physically with

a fluxon, or isolated magnetic vortex, in the junction (e.g., Ref. 17). If we consider a one-dimensional Josephson junction with external field in the x direction only, then the single soliton solution, in the nonrelativistic limit, is given by $\Delta\gamma(y,t)=\phi(y-vt)$, where

$$\phi(y)=4\tan^{-1}[\exp(-y/\lambda_J)] , \tag{2.3}$$

and $v \ll \bar{c}$ is the fluxon velocity. The kink (or "shelf") solution (2.3) goes from 2π to zero as y goes from $-\infty$ to ∞. The kink solution (2.3) and the corresponding Josephson current density

$$J_z(y,z=0)=2J_0\tanh(y/\lambda_J)\mathrm{sech}(y/\lambda_J) \tag{2.4}$$

are plotted as a function of distance y/λ_J in Fig. 3. (In Fig. 3 the phase difference and Josephson current have been normalized by dividing by 2π and J_0, respectively.) The magnetic field corresponding to the fluxon solution (2.3) is given by

$$b_x(y,z=0)=b_0\,\mathrm{sech}(y/\lambda_J) , \tag{2.5}$$

where $b_0 \equiv \hbar c/ed\lambda_J$. We see that for a single Josephson junction there is only one length scale, λ_J, characterizing the spatial variation of $J_z(y,z=0)$ and $b_x(y,z=0)$. The peak value of $J_z(y,z=0)$ occurs at $y \simeq 0.88\lambda_J$, and for large values of y both $J_z(y,z=0)$ and $b_x(y,z=0)$ vary as $\exp(-y/\lambda_J)$.

The rate of dissipation of energy per unit length as a vortex moves through the insulating region of a one-dimensional junction is

$$\frac{1}{R'}\left[\frac{\hbar}{2e}\right]^2\int_{-\infty}^{\infty}\left[\frac{\partial\Delta\gamma(y,t)}{\partial t}\right]^2 dy , \tag{2.6}$$

where $R'=\rho d_i$ is the contact resistivity. Expression (2.6) follows from considering the Ohmic currents produced in the junction barrier by the induced electric field as the vortex moves. We can find a phenomenological viscous drag coefficient η by equating (2.6) to ηv^2. By using the fluxon solution (2.3) in (2.6) we then obtain

$$\eta=\frac{2\phi_0^2}{\pi^2c^2\lambda_J R'} . \tag{2.7}$$

The result (2.7) was first obtained by Lebwohl and Stephen,[22] who also calculated the viscous drag coefficient for N fluxons moving uniformly in a one-dimensional junction.

III. JOSEPHSON-COUPLED LAYER MODEL FOR ANISOTROPIC HIGH-T_c SUPERCONDUCTORS

In Ref. 23 a model for anisotropic high-temperature copper oxide superconductors was developed from the point of view of an array of Josephson-coupled superconducting blocks. When the blocks are fused in the a and b directions, but weakly coupled in the c direction, a layer model results which is similar to that of Lawrence and Doniach.[24] The Lawrence and Doniach model has been extended, e.g., in Refs. 5, 25, and 26. Bulaevskii *et al.* also considered Josephson-coupled layered superconducting structures.[27–31] We wish to consider in addition the vortex structure close to the core region.

The layer model we use is an infinite stack of parallel superconducting layers [see Fig. 4] separated by insulating layers centered on the planes $z=z_n$, where $z_n=ns$ ($n=0,\pm1,\pm2,\ldots$). The length s is the sum of the superconductor layer thickness d_s and the junction barrier thickness d_i. We assume that only a single vortex is present in the model. It is located in the $n=0$ layer and is parallel to the x axis, so that $\mathbf{b}(y,z)=\hat{x}b(y,z)$.

The relation between the magnetic field of the vortex and the gauge-invariant phase difference $\Delta\gamma_n(y)$ of the superconducting wave function across layers n and $n+1$ can be found by integrating the vector potential

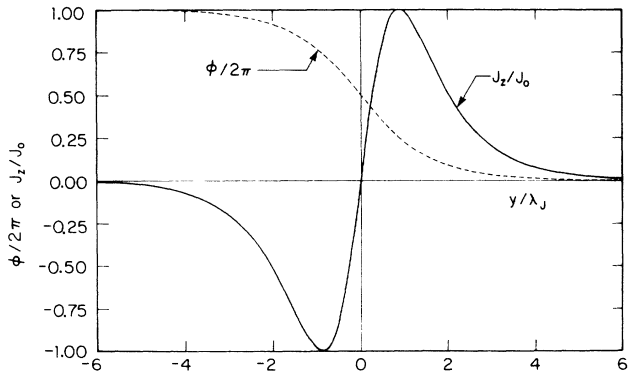

FIG. 3. Single soliton (fluxon) solution [Eq. (2.3)] of the 1D sine-Gordon equation for the normalized gauge-invariant phase difference $\phi/2\pi$ (dashed) and the resulting normalized Josephson tunneling current density J_z/J_0 (solid), plotted as functions of y. The maximum Josephson current occurs at $y=-\lambda_J\ln(\tan\pi/8)\simeq 0.88\lambda_J$.

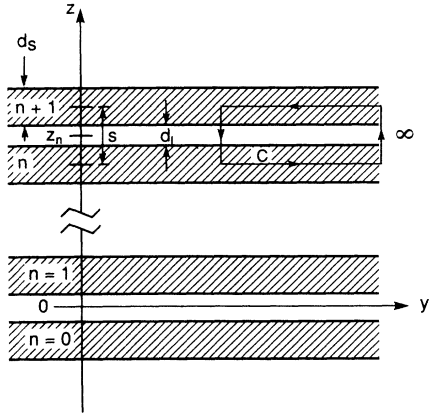

FIG. 4. Geometry of the Josephson-coupled layer model. The insulating layers of thickness d_i alternate with superconducting layers (crosshatched) of thickness d_s. The middle of the insulating layers are in the planes $z_n=ns$ ($n=0,\pm1,\pm2,\ldots$), where $s=d_i+d_s$. The rectangular contour C parallel to the y-z plane with a pair of opposite sides in superconducting layers n and $n+1$ is used to compute the magnetic flux in Eq. (3.2).

$$a_i = -\frac{4\pi\lambda_s^2}{c} j_i - \frac{\phi_0}{2\pi}\frac{\partial\gamma}{\partial x_i} \quad (i=1,2,3=x,y,z) \tag{3.1}$$

around a rectangular contour C, as shown in Fig. 4. This contour is parallel to the y-z plane, with a pair of opposite sides in the n and $n+1$ superconducting layers. Here $\mathbf{j}$ is the supercurrent density, we set $\Delta\gamma_n = \gamma_n - \gamma_{n+1} - (2\pi/\phi_0)\int_n^{n+1}\mathbf{a}\cdot d\mathbf{l}$, and the flux quantum $\phi_0 \equiv hc/2e$. The penetration depth λ_s appearing in Eq. (3.1) is that of individual superconducting layers and is assumed to be isotropic. The Josephson tunneling current density is given by the relation $J_z = J_0 \sin\Delta\gamma_n(y)$. We have the magnetic flux within the semi-infinite contour as

$$\Phi = s\int_y^\infty dy'\, b(y',z) = \int_C \mathbf{a}\cdot d\mathbf{l} \ . \tag{3.2}$$

By using the expression (3.1) in (3.2), performing the integrations, and then differentiating with respect to y we have

$$b(y,z) = -\frac{\phi_0}{2\pi s}\frac{\partial}{\partial y}\Delta\gamma_n(y) - \frac{4\pi\lambda_s^2 d_s}{cs}\frac{\partial}{\partial y}J_z(y,z) + \frac{4\pi\lambda_s^2}{cs}[j_y(y,z_{n+1}) - j_y(y,z_n)] \ . \tag{3.3}$$

By taking into account the relation $sJ_y = d_s j_y$ between the current densities and converting the difference in supercurrent densities in adjacent layers occurring in (3.3) to a partial derivative with respect to z, we have

$$-\frac{\phi_0}{2\pi s}\frac{\partial}{\partial y}\Delta\gamma_n(y) - \frac{4\pi\lambda_s^2 d_s}{cs}\frac{\partial}{\partial y}J_z(y,z) + \frac{4\pi\lambda_b^2}{c}\frac{\partial}{\partial z}J_y(y,z) = b(y,z) \ , \tag{3.4}$$

where $\lambda_b^2 \equiv (s/d_s)\lambda_s^2$. By linearizing the Josephson current relation to $J_z(y,z) \approx J_0\Delta\gamma_n(y)$, we obtain

$$-\frac{4\pi}{c}\lambda_c^2\frac{\partial J_z}{\partial y}(y,z) + \frac{4\pi}{c}\lambda_b^2\frac{\partial J_y}{\partial z}(y,z) = b(y,z) \ , \tag{3.5}$$

with $\lambda_c^2 = c\phi_0/8\pi^2 sJ_0 + \lambda_s^2 d_s/s$. Using Ampere's law $\mathbf{J} = (c/4\pi)\nabla\times\mathbf{b}$, we obtain from (3.5) an anisotropic London equation

$$\lambda_c^2\frac{\partial^2 b}{\partial y^2} + \lambda_b^2\frac{\partial^2 b}{\partial z^2} = b(y,z) \ . \tag{3.6}$$

For a single vortex centered on the origin, we know by the London model[7] that the solution of Eq. (3.6) at large distances is given by

$$b(y,z) = \frac{\phi_0}{2\pi\lambda_b\lambda_c}K_0(\tilde{\rho}), \quad \tilde{\rho}^2 \equiv \tilde{y}^2 + \tilde{z}^2 \ , \quad \tilde{y} \equiv y/\lambda_c, \quad \tilde{z} \equiv z/\lambda_b \ , \tag{3.7}$$

where K_p is a modified Bessel function of the second kind of order p. This result obtains in the large-κ limit, which is the case for the known high-T_c superconductors. An improved solution to Eq. (3.4) can be obtained by extending the use of the variational model for a vortex core in a type-II superconductor.[32] By minimizing the free energy with respect to a core-radius parameter, it is found that, to an excellent approximation when $s \ll \lambda_b$,

$$b(y,z) = \frac{\phi_0}{2\pi\lambda_b\lambda_c}K_0(\tilde{R}) \ , \tag{3.8}$$

where

$$\tilde{R} \equiv (\tilde{x}_0^2 + \tilde{y}^2 + \tilde{z}^2)^{1/2}, \quad \tilde{y} \equiv y/\lambda_c \ , \quad \tilde{z} \equiv z/\lambda_b, \quad \tilde{x}_0 \equiv s/2\lambda_b \ . \tag{3.9}$$

An alternative derivation of the result (3.8) for the magnetic field and the gauge-invariant phase difference is given in Sec. IV. In that section we derive an analog of the sine-Gordon equation, which we call the sine-Bessel equation, and discuss the picture of the vortex core structure that emerges from it.

Figure 5 provides a sketch of the supercurrent distribution around a single vortex located in the barrier region of the central Josephson junction. For the component of the supercurrent density pointing in the b direction, the length scale for exponential decay along the z (c) axis is set by the penetration depth λ_b. Similarly, for the component pointing in the c direction, the length scale for decay along the y (b) axis is set by λ_c. The streamlines of the supercurrent, which also represent contours of constant magnetic field, are elliptical except for the zigzags due to the intervening insulating layers.

For the central junction (at $z=0$), by using Eq. (3.8), Ampere's law, and the Josephson relation $J_z = J_0\sin\Delta\gamma_0$, we have the gauge-invariant phase difference as

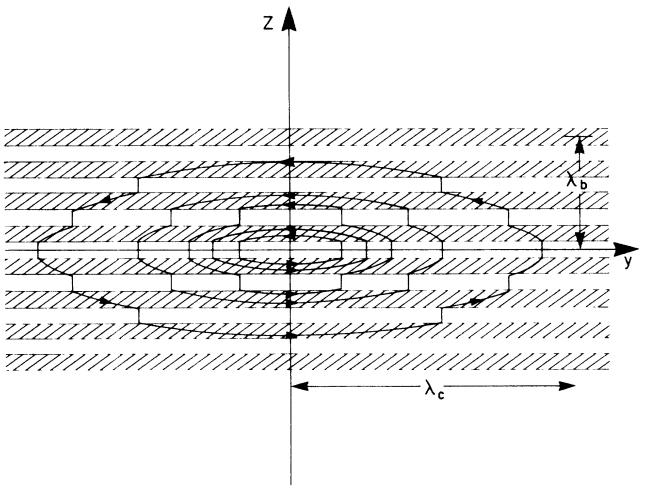

FIG. 5. Sketch of the supercurrent distribution around a single vortex in the barrier region of the central Josephson junction in an infinite layer model of an anisotropic high-T_c superconductor. The vortex is parallel to the x axis (a direction). The London penetration depths λ_c and λ_b give the scale for the decay of the supercurrent in the y (b) and z (c) directions, respectively. The streamlines of the supercurrent, which also represent contours of constant magnetic field, would be ellipses in the absence of the intervening insulating layers.

$$\Delta\gamma_0(y)=\sin^{-1}\left[\frac{(s/\lambda_b)K_1[(\tilde{x}_0^2+\tilde{y}^2)^{1/2}]\tilde{y}}{(\tilde{x}_0^2+\tilde{y}^2)^{1/2}}\right] . \quad (3.10)$$

For very small values of $\tilde{y}$ in (3.10), we can use the asymptotic from $K_1(x)\sim 1/x$, for x near zero, to write the phase difference as

$$\Delta\gamma_0(y)=\pi-2\tan^{-1}(\tilde{y}/\tilde{x}_0), \quad |\tilde{y}|\ll 1 . \quad (3.11)$$

For junctions with $n\neq 0$, the phase difference found by linearizing the Josephson relation and using Ampere's law is

$$\Delta\gamma_n(y)=\frac{s}{\lambda_b}K_1(\tilde{R})\frac{\tilde{y}}{\tilde{R}} \quad (n\neq 0) . \quad (3.12)$$

These expressions for the gauge-invariant phase difference will be applied in the calculation of the viscous drag coefficient in Sec. V.

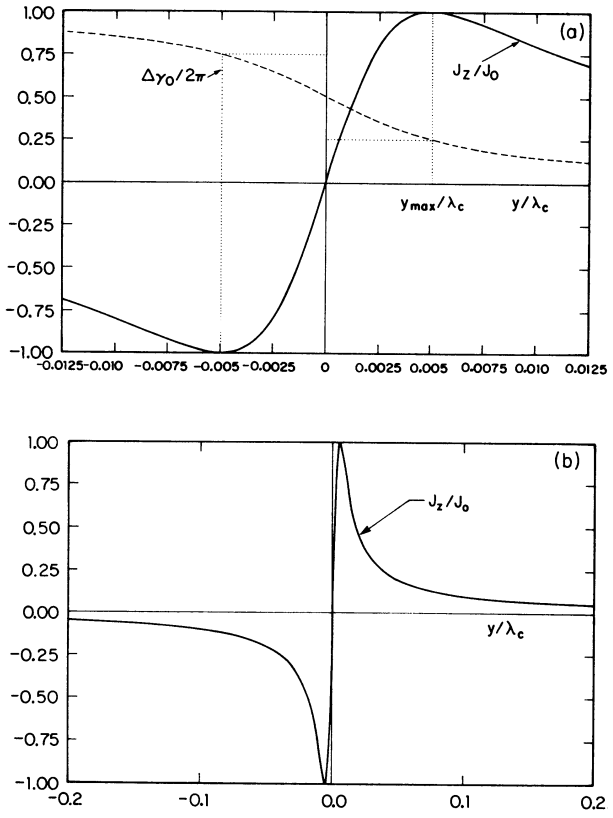

FIG. 6. (a) Normalized phase difference $\Delta\gamma_0/2\pi$ (dashed) of Eq. (3.11) and the resulting normalized Josephson current density J_z/J_0 (solid) in the core region of the central junction are plotted as a function of distance y/λ_c. In this figure, $\tilde{x}_0$ has been set to 1/200. The maximum of the Josephson current density occurs at $y_{max}=\tilde{x}_0\lambda_c=(s/2\lambda_b)\lambda_c$, where $\Delta\gamma_0=\pi/2$. (b) Normalized Josephson current density $J_z/J_0=\sin\Delta\gamma_0$ is plotted as a function of y/λ_c for distances in the central junction exceeding the core size y_{max}/λ_c. By Eq. (3.10), for distances large compared to the core size, the Josephson current density decreases exponentially over the scale of λ_c.

In Eqs. (3.8)–(3.12), $\tilde{x}_0$ serves as a dimensionless vortex core radius. Equations (3.10) and (3.11) give the distance at which the Josephson current reaches its maximum (J_0) in the central junction as $\tilde{y}_{max}=\tilde{x}_0$ or $y_{max}=(s/2\lambda_b)\lambda_c$. We note that for temperatures below the crossover temperature the core does not correspond to a region of suppressed order parameter, but is rather the region in which the magnitude of the Josephson current varies from zero to its maximum value (J_0) (see Fig. 6). That is, for $\xi_c \lesssim s/2$ the continuum description for b and $\Delta\gamma_n$ loses its validity, and the vortex, which fits between neighboring superconducting layers, behaves as a Josephson vortex rather than an Abrikosov vortex. In the z direction the core radius is $\tilde{z}=\tilde{x}_0$ or $z=s/2$. The continuum description for b or $\Delta\gamma_n$ ceases to be valid at distances in the z direction comparable to the layer spacing. If s were less than ξ_c, then we would have to consider suppression of the amplitude of the order parameter, but we are interested in the opposite case $s>\xi_c$ here. As s is on the order of 10 Å for a high-T_c superconductor, this distance is clearly much less than the penetration depths λ_b and λ_c. Typically, $\tilde{x}_0=s/2\lambda_b$ is of the order of the reciprocal of the Ginzburg-Landau parameter κ, or approximately 10^{-2} in a high-T_c superconductor.

For the central junction ($n=0$), the normalized phase difference $\Delta\gamma_0/2\pi$ (dashed) of Eq. (3.11) and the resulting normalized Josephson current density J_z/J_0 (solid) in the core region are plotted as a function of distance y/λ_c in Fig. 6(a). In this figure, $\tilde{x}_0$ has been set to 1/200. This small but representative value of $\tilde{x}_0$ means that the transition region for the phase difference and Josephson current is very small on the length scale of the penetration depth λ_c. The maximum of the Josephson current density occurs at $y_{max}=\tilde{x}_0\lambda_c=(s/2\lambda_b)\lambda_c$.

In Fig. 6(b) the normalized Josephson current density $J_z/J_0=\sin\Delta\gamma_0$ is plotted as a function of y/λ_c for distances in the central junction exceeding the core size y_{max}/λ_c. For distances large compared to the core size, J_z/J_0 drops off very rapidly. Indeed, from Eq. (3.10), we have that the Josephson current density decreases exponentially over the scale of λ_c.

For the Josephson-coupled layer model, we see that there are two length scales required to characterize the spatial variation of $J_z(y,z=0)$ and $b(y,z=0)$. The peak value of $J_z(y,z=0)$ occurs at $y=s\lambda_c/2\lambda_b$, while for large values of y, both $J_z(y,z=0)$ and $b(y,z=0)$ are dominated by the exponential $\exp(-y/\lambda_c)$. The existence of two length scales to characterize J_z and b is in contrast to the single Josephson junction reviewed in Sec. II.

IV. SINE-BESSEL EQUATION AND VORTEX CORE STRUCTURE

In analogy to the sine-Gordon equation for a single Josephson junction, there is a differential equation governing the gauge-invariant phase difference for the Josephson-coupled layer model. Because of the form of this equation, which combines aspects of the Bessel equation and the static sine-Gordon equation, we have termed

it the sine-Bessel equation. The derivation and approximate solution of this equation are the subject of this section. The approximate solution of the sine-Bessel equation is made possible by the anisotropy of the superconductor together with the very small size of the stacking periodicity s compared to the penetration depth λ_b.

We recall that Eq. (3.4), found by calculating the magnetic flux through a rectangular contour across adjacent superconducting layers, is an exact relation between the gauge-invariant phase difference, the supercurrent, and the magnetic field of the vortex. We also recall that the linear equations (3.5) and (3.6) are approximate equations. Here we refrain from linearizing (3.4) in order to investigate the vortex core region. Using the Josephson relation for J_z, we can write Eq. (3.4) in the form

$$b(y,z)=-\frac{4\pi J_0}{c}\left[\frac{c\phi_0}{8\pi^2 s J_0}+\frac{\lambda_s^2 d_s}{s}\cos\Delta\gamma_n(y)\right]\times\frac{\partial\Delta\gamma_n(y)}{\partial y}+\frac{4\pi\lambda_b^2}{c}\frac{\partial J_y}{\partial z}(y,z)\ . \tag{4.1}$$

By the inequality $\lambda_c^2 \gg \lambda_s^2 d_s/s$ we can neglect the term with $\cos\Delta\gamma_n$ on the right-hand side of Eq. (4.1). This approximation is well justified for high-T_c superconductors, since, for example, in $YBa_2Cu_3O_{7-\delta}$,[33,34] we have $\lambda_c:\lambda_b=5.5:1$. The resulting equation together with the Josephson relation provides us with the two basic first-order differential equations

$$-\frac{\phi_0}{2\pi s}\frac{\partial}{\partial y}\Delta\gamma_n(y)+\frac{4\pi\lambda_b^2}{c}\frac{\partial}{\partial z}J_y(y,z)=b(y,z)\ , \tag{4.2a}$$

$$J_z(y,z)=J_0\sin\Delta\gamma_n(y)=-\frac{c}{4\pi}\frac{\partial b}{\partial y}(y,z)\ . \tag{4.2b}$$

Motivated by Eq. (3.6), we look for b in the form $b=b(\tilde\rho)$, where $\tilde\rho$ is defined in Eq. (3.7). That is, we assume that the contours of constant b are ellipses. We are most interested in the central junction where $z=0$, $\tilde\rho=\tilde y$, and set $\tilde b\equiv b(2\pi s\lambda_c/\phi_0)$. In this case Eq. (4.2) gives

$$\tilde b(\tilde\rho)=-\frac{\partial\Delta\gamma_0}{\partial\tilde\rho}+\frac{1}{\tilde\rho}\frac{\partial\tilde b}{\partial\tilde\rho}\ , \tag{4.3a}$$

$$\frac{\partial\tilde b}{\partial\tilde\rho}=-\sin\Delta\gamma_0\ . \tag{4.3b}$$

The coupled equations (4.3) are the focus of this section. By eliminating the scaled magnetic field $\tilde b$ from (4.3), we obtain an equation referred to as the sine-Bessel equation:

$$\frac{\partial^2\phi}{\partial x^2}+\frac{1}{x}\frac{\partial}{\partial x}\sin\phi-\left[1+\frac{1}{x^2}\right]\sin\phi=0\ , \tag{4.4}$$

where $\phi\equiv\Delta\gamma_0$ and $x\equiv\tilde\rho$. We anticipate a static kink solution for ϕ from (4.4) in analogy with the single junction case. For the sine-Bessel equation (4.4) we have the boundary conditions $\phi=2\pi$ at $x=-\infty$ and $\phi=0$ at $x=\infty$. Because of the presence of the vortex there, we should also have $\phi=\pi$ at $x=0$. By the fluxoid quantization relation

$$\int\int b(y,z)dy\,dz=2\pi\lambda_b\lambda_c\int_0^\infty xb(x)dx=\phi_0 \tag{4.5}$$

and Eq. (4.3b), there results the normalization condition

$$\int_0^\infty x^2\sin\phi\,dx=2s/\lambda_b\ , \tag{4.6}$$

on the solution of the sine-Bessel equation. We remark that the term of unity in the coefficient of the last term of (4.4) prevents this equation from being scale invariant in the independent variable x. In addition, this term prevents a straightforward first integration of the sine-Bessel equation. We argue below that this term is insignificant for small x. For small ϕ the linearized version of Eq. (4.4) holds, giving a Bessel equation whose solution is $\phi\approx(s/\lambda_b)K_1(x)$, where the constant is set by the normalization condition (4.6). This result gives that $\tilde b\approx(s/\lambda_b)K_0(x)$ for small ϕ, i.e., outside the core region. On the other hand, when dealing with the behavior of the phase difference for small x, it appears simplest to deal directly with the first-order equation (4.3a). By the normalization condition the value of b in the core region is controlled by a ratio of lengths of order $2s/\lambda_b$. This ratio is the value at which the logarithmic divergence of (3.7) will be cut off. We may then estimate $b(0)$ as $b(0)\approx(\phi_0/2\pi\lambda_b\lambda_c)\ln(\lambda_b/s)$ so that $\tilde b(0)\approx(s/\lambda_b)\ln(\lambda_b/s)\ll 1$.

For small x, we let $\phi(x)=\pi-\alpha(x)$ [so that $\alpha(0)=0$] and substitute into (4.3a), neglecting $\tilde b$. The simple equation $d\alpha/dx+(\sin\alpha)/x=0$ may be integrated to yield $\alpha=2\tan^{-1}(x/\tilde x_0)$, where $\tilde x_0$ is a constant of integration. This result for α gives, when inserted into Eq. (4.3b), the expression $\tilde b(x)=-\tilde x_0\ln(x^2+\tilde x_0^2)$. We find $\tilde x_0$ by matching this form of $\tilde b$ to its form for larger values of x, i.e., $\tilde b=(s/\lambda_b)\ln(1/x)$. This gives $\tilde x_0=s/2\lambda_b\ll 1$. This small value of $\tilde x_0$ indicates that the approximations used are self-consistent. In particular, the value of $\tilde b$ in the core is negligible compared to the right-hand side of Eq. (4.3a). We recall that since we are considering the central junction, $x\equiv\tilde\rho=\tilde y$. By employing the variable $\tilde R^2\equiv\tilde\rho^2+\tilde x_0^2$ of Eq. (3.9), we obtain the expressions (3.10)–(3.12) as stated in Sec. III.

V. CALCULATION OF VISCOUS DRAG COEFFICIENT

We consider the motion of a single vortex experiencing a viscous drag force per unit length, $-\eta v$, where v is the vortex velocity, assumed to be constant. The flux flow viscosity is to be calculated by equating the energy dissipation rate per unit length to ηv^2. For an applied current I, flowing in the z direction, the dissipation rate per unit area across junction n is

$$\frac{IV}{A}=J_zV=R'J_z^2=\frac{1}{R'}V^2\ , \tag{5.1}$$

where $R'\equiv RA=\rho_c s$ is the contact resistivity in the c direction. The voltage across the nth junction is given by

$$V=\frac{\hbar}{2e}\frac{\partial\Delta\gamma_n(y,t)}{\partial t}=-v\frac{\hbar}{2e}\frac{\partial\Delta\gamma_n(y)}{\partial y}\ , \tag{5.2}$$

where the gauge-invariant phase difference $\Delta\gamma_n(y,t)$ is

taken to be of the traveling-wave form $\Delta\gamma_n(y,t)=\Delta\gamma_n(y-vt)$. Using (5.1) and (5.2), we have the expression

$$\eta_n=\frac{1}{R'}\left[\frac{\hbar}{2e}\right]^2\int_{-\infty}^{\infty}\left[\frac{\partial\Delta\gamma_n(y)}{\partial y}\right]^2 dy\ , \tag{5.3a}$$

as the contribution from the nth junction. The total viscous drag coefficient can be found by summing over all junctions:

$$\eta=\sum_{n=-\infty}^{\infty}\eta_n\ . \tag{5.3b}$$

For the central junction ($n=0$) we use Eq. (3.11) to obtain

$$\eta_0=\frac{1}{R'}\left[\frac{\hbar}{2e}\right]^2\frac{2\pi}{\lambda_c\tilde{x}_0}\ . \tag{5.4}$$

Since it can be shown that the maximum of $\Delta\gamma_n$ decreases with n approximately as $1/2|n|$, we can well approximate η_n for $|n|\geq 1$ by using the asymptotic form of (3.12) valid for small $\tilde{R}$, where the greatest contribution to η occurs. We have

$$\Delta\gamma_n(y)\simeq\frac{2\tilde{x}_0\tilde{y}}{\tilde{R}^2}\quad\text{for } \tilde{R}\ll 1\ . \tag{5.5}$$

By using the form (5.5) we obtain

$$\sum_{\substack{n=-\infty\\ n\neq 0}}^{\infty}\int_{-\infty}^{\infty}\left[\frac{\partial\Delta\gamma_n}{\partial y}\right]^2 dy = \left[\frac{s}{\lambda_b}\right]^2\frac{1}{\lambda_c}\frac{\pi}{2}\frac{1}{\tilde{x}_0^3}\sum_{n=1}^{\infty}\frac{1}{(1+4n^2)^{3/2}}\ , \tag{5.6}$$

where the approximate numerical value of the sum on the right-hand side of (5.6) is 0.113 08. By the use of (5.3b), (5.4), and (5.6), we obtain for the viscous drag coefficient

$$\eta=0.3543\left[\frac{m_b}{m_c}\right]^{1/2}\frac{\phi_0^2}{\rho_c s^2 c^2}\ , \tag{5.7}$$

where the approximate value of the infinite sum of (5.6) and a factor with π have been included in the numerical coefficient, s is the layer periodicity length, and c is the speed of light. The result (5.7) is to be compared to the anisotropic BS model, which in the dirty limit gives[12] $\eta=\phi_0^2/2\pi\xi_b\xi_c c^2\rho_c$. Therefore, we see that the vortex core area $\propto\xi_b\xi_c$ in the anisotropic BS expression has been replaced by an area of order $sy_{\max}\sim s^2\lambda_c/\lambda_b\sim s^2(m_c/m_b)^{1/2}$, due to the superconductor discreteness. Equation (5.7) thus yields the flux flow resistivity

$$\rho_f=2.822\left[\frac{m_c}{m_b}\right]^{1/2}\frac{B}{(\phi_0/s^2)}\rho_c\ , \tag{5.8}$$

for flux density $B\ll B_{c2a}$, current in the c direction, and vortex motion in the b direction.

VI. SUMMARY

In this paper we reviewed the core structure of a straight vortex threading through the insulating barrier of a Josephson junction and the calculation of the viscous drag coefficient when such a vortex moves through the insulating region. Next, we developed the theory for the vortex structure in a Josephson-coupled layer model of a high-T_c superconductor. This model consists of superconducting layers of thickness d_s alternating with insulating layers of thickness d_i, giving a stacking periodicity of $s=d_i+d_s$. This model takes into account the discreteness of the copper oxide planes in a high-T_c material, which is expected to be important when $\xi_c(T)$, the coherence length in the c direction, is less than the lattice parameter c. Our layer model involves a parameter $\tilde{x}_0\equiv s/2\lambda_b$, of the order of the inverse of the Ginzburg-Landau parameter κ, or approximately 10^{-2} in a high-T_c superconductor. This parameter serves as a dimensionless vortex core radius. We noted that for temperatures below the crossover temperature the core does not correspond to a region of suppressed order parameter, but is rather the region in which the magnitude of the Josephson current varies from zero to its maximum value. That is, for $\xi_c\lesssim s/2$ the continuum description for the magnetic field of the vortex and the gauge-invariant phase difference loses it validity, and the vortex, which fits between neighboring superconducting layers, behaves as a Josephson vortex rather than an Abrikosov vortex. For the central junction the maximum value of the Josephson current occurs at $y_{\max}=\tilde{x}_0\lambda_c$. In contrast to the case of a single Josephson junction, this second length is required in addition to λ_c to describe the spatial variation of the magnetic field and Josephson current. We then applied the theory for the vortex structure to compute the viscous drag coefficient η.

We calculated the viscous drag coefficient η for a vortex in a microscopically layered high-T_c superconductor, the vortex being parallel to the a axis, and moving in the b direction under the influence of an applied driving current in the c direction and compared the result to the anisotropic BS model.[12] In the BS model the dissipation that contributes to the viscous drag is concentrated in the vicinity of the vortex core. The anisotropic BS result for the viscous drag coefficient contains a cross-sectional area of the vortex core region proportional to $\xi_b\xi_c$. In contrast, our result (5.7) contains an area proportional to $sy_{\max}\sim s^2(m_c/m_b)^{1/2}$, owing to the discreteness of the high-T_c superconductor. So, as anticipated, if the vortex core region has altered behavior at low temperature due to the atomic scale discreteness of the superconductor's structure, then the corresponding expression for the viscous drag coefficient is also altered.

ACKNOWLEDGMENTS

We thank H. Blackstead, D. K. Finnemore, V. G. Kogan, Z. Hao, and W. Tomasch for helpful discussions. Ames Laboratory is operated for the U.S. Department of Energy by Iowa State University under Contract No. W-7405-Eng-82. This work was supported by the Director for Energy Research, Office of Basic Energy Sciences.

[1]V. L. Ginzburg, Zh. Eksp. Teor. Fiz. **23**, 236 (1952).
[2]C. Caroli, P. G. de Gennes, and J. Matricon, Phys. Kondens. Mater. **1**, 176 (1963).
[3]L. P. Gor'kov and T. K. Melik-Barkhudarov, Zh. Eksp. Teor. Fiz. **45**, 1493 (1963) [Sov. Phys.—JETP **18**, 1031 (1964)].
[4]E. I. Katz, Zh. Eksp. Teor. Fiz. **56**, 1675 (1969) [Sov. Phys.—JETP **29**, 897 (1969)]; **58**, 1471 (1970) [**31**, 787 (1970)].
[5]R. A. Klemm, A. Luther, and M. Beasley, Phys. Rev. B **12**, 877 (1975).
[6]D. R. Tilley, G. J. Van Gurp, and C. W. Berghout, Phys. Lett. **12**, 305 (1964).
[7]V. G. Kogan, Phys. Rev. B **24**, 1572 (1981).
[8]V. G. Kogan and J. R. Clem, Phys. Rev. B **24**, 2497 (1981).
[9]N. R. Werthamer, E. Helfand, and P. C. Hohenberg, Phys. Rev. **147**, 295 (1966).
[10]U. Welp *et al.*, Phys. Rev. Lett. **62**, 1908 (1989).
[11]J. Bardeen and M. J. Stephen, Phys. Rev. A **140**, 1197 (1965).
[12]Z. Hao and J. R. Clem (unpublished).
[13]D. E. Farrell *et al.*, Phys. Rev. Lett. **64**, 1573 (1990).
[14]U. Welp *et al.*, Phys. Rev. B **40**, 5263 (1989).
[15]L. P. Gor'kov and N. B. Kopnin, Usp. Fiz. Nauk **116**, 413 (1975) [Sov. Phys. Usp. **18**, 496 (1976)].
[16]V. M. Genkin and A. S. Mel'nikov, Zh. Eksp. Teor. Fiz. **95**, 2170 (1989).
[17]A. Barone and G. Paterno, *Physics and Applications of the Josephson Effect* (Wiley, New York, 1982).
[18]I. O. Kulik and I. K. Yanson, *The Josephson Effect in Superconductive Tunneling Structures* (Israel Program for Scientific Translations Ltd., Jerusalem, 1972).
[19]K. K. Likharev, *Dynamics of Josephson Junction and Circuits* (Gordon and Breach, New York, 1986).
[20]S. L. Miller *et al.*, Phys. Rev. B **31**, 2684 (1985).
[21]D. W. McLaughlin and A. C. Scott, Phys. Rev. A **18**, 1652 (1978).
[22]P. Lebwohl and M. J. Stephen, Phys. Rev. **163**, 376 (1967).
[23]J. R. Clem, Physica C **162-164**, 1137 (1989).
[24]W. Lawrence and S. Doniach, *Proceedings of the Twelfth International Conference on Low Temperature Physics,* edited by E. Kanda (Academic Press of Japan, Kyoto, 1971), p. 361.
[25]R. A. Klemm, Solid State Commun. **46**, 705 (1983).
[26]T. Koyama, N. Takezawa, and M. Tachiki, Physica C **168**, 69 (1990).
[27]L. N. Bulaevskii, Usp. Fiz. Nauk **116**, 449 (1975) [Sov. Phys. Usp. **18**, 514 (1976)].
[28]L. N. Bulaevskii, V. L. Ginzburg, and A. A. Sobyanin, Zh. Eksp. Teor. Fiz. **94**, 355 (1988) [Sov. Phys. JETP **68**, 1499 (1988)].
[29]L. N. Bulaevskii, Zh. Eksp. Teor. Fiz. **64**, 2241 (1973) [Sov. Phys.—JETP **37**, 1133 (1973)].
[30]L. N. Bulaevskii, Zh. Eksp. Teor. Fiz. **66**, 2212 (1974) [Sov. Phys.—JETP **39**, 1090 (1974)].
[31]L. N. Bulaevskii, Zh. Eksp. Teor. Fiz. **65**, 1278 (1973) [Sov. Phys.—JETP **38**, 634 (1974)].
[32]J. R. Clem, J. Low Temp. Phys. **18**, 427 (1975).
[33]G. J. Dolan *et al.*, Phys. Rev. Lett. **62**, 2184 (1989).
[34]L. Ya. Vinnikov *et al.*, Pis'ma Zh. Eksp. Teor. Fiz. **49**, 71 (1989) [JETP Lett. **49**, 83 (1989)].